Large area colloidal photonic crystals for light trapping in flexible organic photovoltaic modules applied using a roll-to-roll Langmuir-Blodgett method

Mikhail Parchine[a,*], Tomas Kohoutek[a], Maria Bardosova[a], Martyn E. Pemble[a,b]

[a] Tyndall National Institute, UCC, Lee Maltings, Dyke Parade, Cork, Ireland
[b] Department of Chemistry, University College Cork, Cork, Ireland

ABSTRACT

For the first time, the application of large-area 2D colloidal photonic crystals for light trapping in flexible OPV modules is demonstrated via the study of a broad range of light trapping structures deposited simply and cheaply using our novel roll-to-roll Langmuir–Blodgett technique. Commercially available flexible OPV modules with a size of 10 cm × 14 cm were used. Colloidal silica spheres with diameters ranging from 50 nm to 740 nm were used for the photonic crystal fabrication. The photonic structures made from SiO_2 spheres with diameters of 50 nm and 120 nm demonstrate good antireflective properties in the visible and near-infrared spectral range, which have a pronounced positive effect on the photocurrent and the power conversion efficiency in OPV modules at all angles of the light incidence. The 2D photonic crystals made from SiO_2 spheres with diameters of 600 nm and 740 nm show strong diffractive scattering of incident light in the forward direction, which results in significant light trapping effects in the OPV modules which again gives rise to an improvement in the cell characteristics. The observed light trapping effects vary only slightly with angle of incidence, suggesting that such photonic crystal layers could be of direct benefit in terms of the response of the OPV modules without the need to track the sun position as it moves across the sky.

1. Introduction

Organic photovoltaic (OPV) cells are promising candidates for future photovoltaic technology because they are low cost, low weight, and can easily be fabricated on flexible substrates by high-volume roll-to-roll deposition or printing methods [1,2]. However, for optimal performance the photoactive layers must be very thin (~ 100 nm) due to the low charge carrier mobilities in the active layers and as a result, poor charge extraction efficiencies are currently observed in OPV cells. Under such circumstances the light absorption is incomplete in these thin photoactive layers. Therefore, different light trapping strategies have been studied designed to improve the light absorption in the photoactive layers which will enhance the power conversion efficiency of OPV cells [3–5]. Among these techniques there are antireflective layers [6,7], electrodes with diffractive grating nanostructures [8–10], and photonic crystal structures fabricated inside OPV cells [11]. Antireflective coatings reduce unnecessary reflection of incident light from the interfaces, increasing the intensity of light going into the photoactive layer of the OPV cells. Therefore, more photocurrent will be generated, enhancing the total power conversion efficiency of OPV cells. In Ref. [6] a 13% relative enhancement in power conversion

efficiency (from 1.8% to 2.05%) was demonstrated in a small size (0.16 cm^2) polymer solar cell (P3HT:PCBM) by using nanostructured antireflective coating made from silica nanospheres which reduced reflectance from ITO coated glass substrate from 10% to 7%. Similarly, moth eye antireflective coatings applied on ITO coated glass substrate have demonstrated reduction of the reflection losses by 3 – 4%, which can improve the efficiency of a polymer solar cell (P3HT:PCBM) with an active area of 1 cm^2 by 2.5–3% [7]. This enhancement was observed for all angles of incidence. Electrodes with light diffraction grating structures can significantly increase the photocurrent in OPV cells due to diffractive scattering of light and plasmonic effects. In Ref. [8] back electrodes with 1D and 2D grating structures were fabricated by using soft nanoimprint lithography of the active layer (P3HT:PCBM) followed by evaporation of the aluminium electrode. Optimising the period and depth of the grating structures, an enhancement of short-circuit current density of 10% was obtained for the 1D grating and 14% for the 2D grating with corresponding increase of the power conversion efficiency of 14% (from 3.6% to 4.1%) and 19% (from 3.6% to 4.3%) for 1D and 2D gratings, respectively. A significant enhancement of the efficiency by 19% (from 3.09% to 3.68%) was observed in an inverted polymer solar cells (P3HT:PCBM) with a nanoimprinted silver back grating [9].

Very effective light trapping was demonstrated in polymer solar cells (P3HT:PCBM, 0.04 cm^2) by using top ITO electrodes with nanoimprinted light-diffraction structures [10]. These structures formed two-dimensional hexagonal arrays with different periods of 1200, 800, and 600 nm. The best enhancement result was achieved on a solar cell with a structure period of 800 nm: the short-circuit current density was increased by 52% from 7.07 to 10.76 mA/cm^2 and the power conversion efficiency was increased by 42% from 2.75% to 3.92%. In Ref. [11] a photonic crystal (PhC) approach was applied for light trapping inside the OPV cells. A nanoimprint process was used to directly pattern the active layer (P3HT:PCBM) in the shape of a 2D PhC slab: an hexagonal lattice of holes was imprinted. By optimising the PhC structure the photonic absorption within the active layer was improved due to light coupling into slow Bloch modes near the optical band gap of P3HT:PCBM blend.

One of the unique properties of photonic crystals (PhCs) is that they possess a photonic bandgap due to the periodic variation of refractive index in three, two or one dimensions. Therefore, we can distinguish 3D, 2D or 1D PhCs. The unique properties of PhCs which allow manipulation of light with certain wavelengths and in certain directions have been employed in optoelectronics [12], sensors [13], and photovoltaics [14,15]. In photovoltaics, for example, 3D colloidal PhCs fabricated from silica nanospheres (with a diameter of 250 nm) can be used as solar concentrators for building-integrated photovoltaics [14] and a 2D colloidal PhC fabricated from silica spheres (with a diameter of 700 nm) was found to be quite effective as a light trapping layer in small size (0.25 cm^2) thin film (250 nm) a-Si:H solar cells [15]. The average relative enhancement observed in solar cells with this light trapping layer for the short circuit current was 8.5% and for the efficiency was 7.0%.

Of note in developing an appropriate light trapping strategy for OPV cells is that the fabrication processes devised for the formation of any light trapping photonic structures must be compatible with the large scale manufacture of OPV modules based on roll-to-roll (R2R) coating and the use of such deposition or printing methods under ambient conditions.

Colloidal photonic crystals (PhCs) can be easily fabricated via the self-assembly of colloidal monodisperse spheres of dielectric materials by using a controlled evaporation methods [16], spin coating [17], doctor blade coating [18], electrospray techniques [19] and the Langmuir-Blodgett (LB) method [20]. Among these methods, the LB method is one of the fastest, most versatile and scalable techniques that allows fabrication of 2D and 3D PhC structures with full control over the number of layers deposited and the composition of each layer allowing in this way creation of PhCs with tuneable optical properties [20–22]. Recently, a R2R LB technique was developed in our laboratory that can be used for the fabrication of large area 2D and 3D colloidal PhCs on flexible polyethylene terephthalate (PET) film [23]. This simple and cheap technology is easy scalable, roll-to-roll compatible, can be used under ambient conditions, and as we demonstrate here, is capable of significantly enhancing the performance of large size flexible OPV modules. An important advantage of this technology for light trapping in OPV cells in comparison with the nanoimprint lithography that it will not lead to degradation or morphology changes in the photoactive layers of OPV cells.

For the first time, the application of large-area 2D colloidal photonic crystals for light trapping in flexible OPV modules is demonstrated. 2D colloidal PhC structures were fabricated on the OPV modules using our R2R LB technique. Colloidal silica spheres with different diameters from 50 nm to 740 nm were used for fabrication of the PhC structures. The choice of this range of diameters for silica spheres can be explained by the fact that colloidal photonic crystal layers made from small size nanospheres (maximum diameter around 150 nm or less) can exhibit good antireflective properties and for larger sized spheres, typically having diameters greater than 500 nm, we can expect strong diffractive scattering of the incident light in the forward direction and coupling of light due to photonic resonances in the 2D arrays of silica spheres which will enhance light absorption in the photoactive layer of the flexible OPV modules. Light trapping properties of the fabricated 2D photonic structures for OPV modules are presented and analysed.

2. Experimental

Commercially available flexible OPV modules (infinityPV ApS) with a size of 10 cm × 14 cm and an active area of 50 cm^2 were used in these experiments. These OPV modules were fabricated on PET foil using ambient R2R printing and coating methods.

Large area 2D colloidal PhCs were deposited on the flexible OPV modules using the R2R LB technique described elsewhere [23]. Colloidal silica spheres with different diameters were used: 50 nm, 120 nm, 210 nm, 350 nm, 600 nm, and 740 nm. Colloidal monodispersed silica spheres were synthesised using a modified Stöber method [24] involving the hydrolysation of tetraethyl orthosilicate (TEOS) in the presence of ethanol, with ammonium hydroxide also present as a catalyst. Each preparation was performed at room temperature under constant magnetic stirring for 24 h, followed by removal of unreacted TEOS and ammonia by repeated centrifuging and washing-sonication cycles in ultrapure water and ethanol [25].

A high resolution scanning electron microscope (HRSEM, Quanta FEG 650, FEI Company) was used to characterize the 2D PhC structures.

Optical transmission spectra of the 2D colloidal PhCs and the OPV modules with and without the light trapping layers were measured using a Mikropack halogen HL2000 white light source having a focused spot size at the sample of 1.5 mm diameter. The transmitted light was collected via an optical fibre to an Ocean Optics HR4000 detector for wavelengths in the VIS-NIR range. A reflection probe (Ocean Optics) was used for reflectance measurements at normal incidence. Spectral analysis was performed using SpectraSuite software. Reflectance measurements were calibrated against a Thor Laboratories ME1-PO1 silver mirror. Transmission calibration was made with respect to air. Transmission spectra of the samples were acquired at the angle of incidence θ = 0° with respect to the normal to the surface of the film. The spectral and spatial repeatability of the optical transmission and reflectance data recorded from the 2D colloidal PhCs was found to be better than 1%. This confirms the high quality of the large area PhC structures fabricated by the R2R LB method. It is important to note also that very good time stability of the optical properties was observed for the 2D PhCs made from silica nanospheres. No significant changes to the transmission and reflection properties of the films concerned were observed over a period of several months. To increase the mechanical stability and robustness of the photonic films and also improve the adhesion to different substrates, they can be coated with a thin layer of optical adhesive using for example, a roll-to-roll slot-die coater, as was demonstrated in ref. [23]. As an alternative approach, large-area flexible colloidal PhC film stickers for light trapping applications have been developed recently in our labs [26].

Photocurrent–voltage (I-V) characteristics of bare OPV modules and OPV modules with different light trapping structures were measured in a solar simulator (Newport) using a Keithley 2430 source meter under ambient atmosphere and simulated solar light, air mass AM 1.5 (1000 W/m^2). The light intensity was calibrated using a reference photovoltaic cell. It was found that the repeatability of the I-V measurements was essentially governed by the stability of the light source, which was better than 1%. For the same lighting conditions identical I-V curves were observed. This is related also to the I_{SC} and PCE parameters. It is important to note that the I-V characteristics of the bare OPV modules were measured first and then the 2D PhC structures were deposited. After that the I-V curves of the OPV modules with different 2D colloidal PhC layers were measured again. The commercial OPV modules have demonstrated very good time stability: after one month no changes in performance was observed.
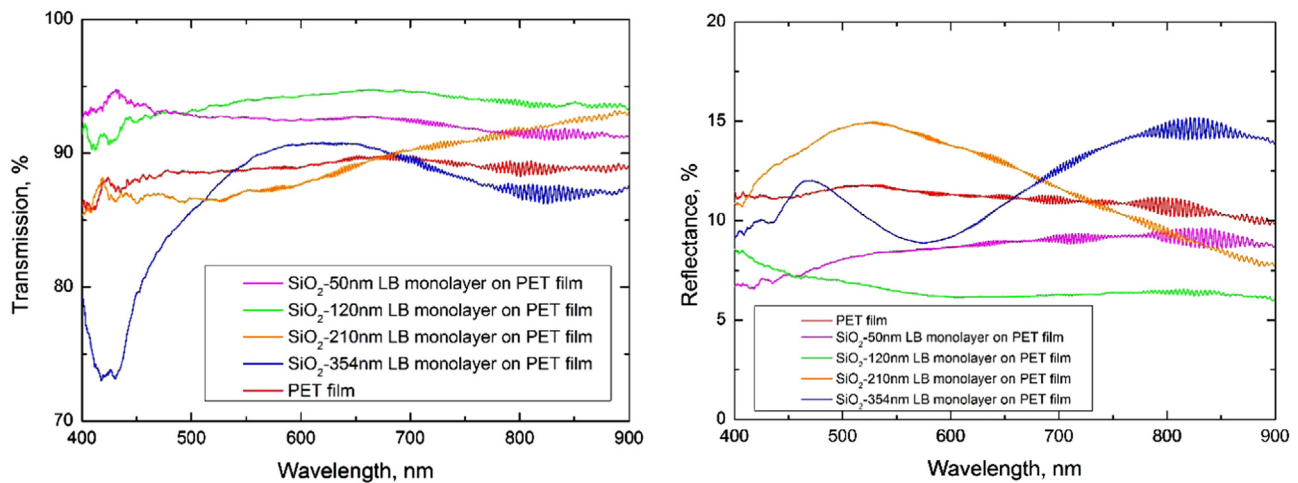
Fig. 1. The optical properties of the 2D PhCs deposited on PET film using the R2R LB technique. The 2D photonic structures made from SiO_2 spheres with diameters of 50 nm and 120 nm demonstrate good antireflective properties in the broad spectral range (VIS-NIR).

3. Results and discussion

We investigated the antireflective properties of 2D colloidal PhCs made by the R2R LB technique from silica spheres with different diameters: 50 nm, 120 nm, 210 nm and 350 nm. First, the optical transmission and reflectance spectra and then the performance parameters of the OPV modules with and without these PhC structures were measured and analysed.

Optical transmission and reflectance spectra of the four different 2D PhC structures deposited on PET film (with a thickness of 50 μm) are presented in Fig. 1. The 2D photonic structures made from silica nanospheres with diameters of 50 nm and 120 nm demonstrate good antireflective (AR) properties in the broad spectral range from visible to near-infrared (VIS-NIR). For example, the reflectance is significantly reduced from 11% to 6% for the layer of 120 nm silica nanospheres, which corresponds to an increase in the transmission from 89% to 94%. The 2D PhC with SiO_2 spheres of 210 nm shows antireflective properties in near-infrared spectral range (> 800 nm). For the 2D PhC layer of 350 nm silica spheres we observed only a small enhancement in transmission and a decrease in reflectance for visible light for wavelengths between 500 nm and 700 nm. At the same time, in the transmission spectrum of this PhC structure (SiO_2 – 350 nm) a strong attenuation of blue light due to diffractive scattering is observed.

The antireflective properties of LB films prepared from silica nanospheres (20 – 110 nm) on glass substrates have been extensively studied and are well known [27,28]. For the optimal antireflective layer, its refractive index can be determined using the formula: $n_{AR} = \sqrt{n_1 n_2}$, where n_1 is the refractive index of surrounding media and n_2 is the refractive index of the substrate. In our case when $n_1 = 1$ (air) and $n_2 = 1.57$ (PET film), the n_{AR} will be equal to 1.253. The effective refractive index of the AR nanospheres layer (SiO_2 50 nm and 120 nm) can be calculated using effective medium theory assuming the volume

fraction of silica nanospheres to be 60.5% for a hexagonally closed packed array of spheres. The refractive index of colloidal silica spheres is 1.43–1.45. Therefore, the effective refractive index of the AR nanospheres layer will be in the range 1.260–1.272. This value is very close to the optimal. Therefore, it is obvious that LB monolayers of silica nanospheres (50–120 nm) deposited on PET film can act as a very good AR layer. It should be mentioned that by mistake in many publications authors are using 74% as the volume fraction value of spheres, which is valid for a 3D hexagonal closed packed structure, but not for a single layer of spheres. Necessarily therefore for 3D structures, the value for the effective refractive index of the AR layer is much higher.

Fig. 2 shows an SEM image and a photograph of the 2D photonic nanostructure of 120 nm SiO_2 spheres deposited on PET film using the R2R LB technique. This layer of silica nanospheres has a total area of 360 cm². On the photograph one can see excellent transparency of the PET film coated with the nanospheres layer. We also measured the reflectance spectra of the bare OPV module and the OPV module with the AR layer of 120 nm SiO_2 spheres. The reflectance spectra are measured on the OPV module where the photoactive layer is present as a coating on the front PET film. These spectra are presented in Fig. 3. As expected, a significant reduction in the reflectance from the PET film is observed.

Fig. 4 presents the photographs and the photocurrent-voltage (I-V) graphs of the OPV modules with and without deposited AR layer (nanospheres SiO_2 120 nm). The I-V characteristics presented in the Fig. 4 are measured in the solar simulator at normal incidence of the light. As one can see from Fig. 4, the short circuit photocurrent (I_{sc}) is increased by 8.3% in the OPV module with AR nanospheres layer. However, the fill factor (FF) is slightly reduced from 56.2% to 55.2%. This can be explained by recombination losses in the photoactive layer which is a little too thick, due to the low charge carrier mobilities for the materials in question, over which we have no control of course, because these are
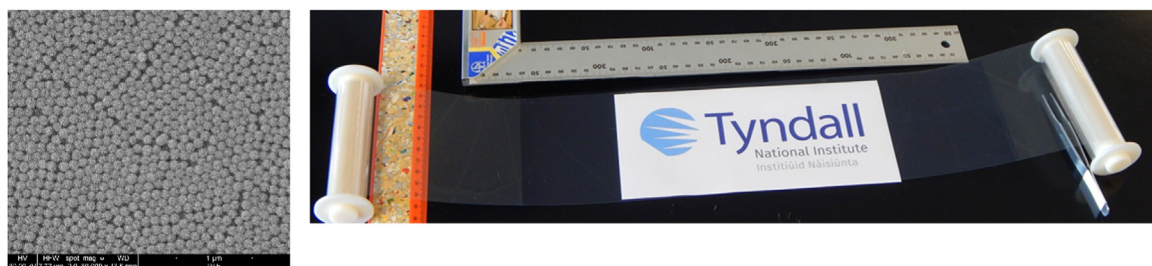

Fig. 2. SEM image (left) and photograph (right) of the antireflective nano-structure (SiO_2 nanospheres with a diameter of 120 nm) deposited on PET film using the R2R LB technique. The total area is 360 cm².
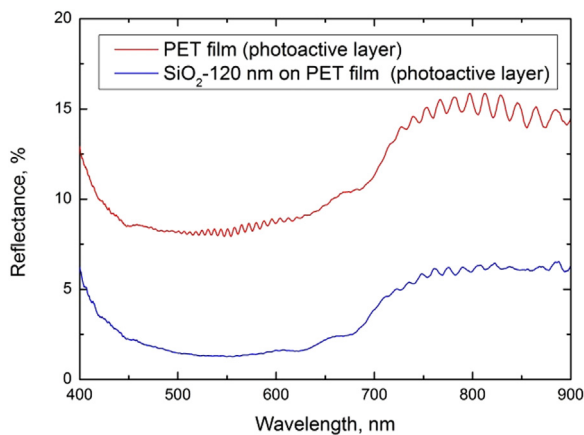
Fig. 3. Reflectance spectra of the bare OPV module (PET film and photoactive layer) and the OPV module with the the AR layer (nanospheres SiO$_2$ 120 nm) deposited by using the R2R LB technique.

commercial OPV structures. This is actually the main limitation factor for the observed enhancement of the power conversion efficiency (PCE) by using the light trapping structures.

The photocurrent and the power conversion efficiency in OPV modules were measured at different angles of the light incidence. The AR layer (nanospheres SiO$_2$ 120 nm) has a pronounced positive effect on photocurrent and efficiency at all angles of the light incidence as shown in Fig. 5. We observed that the short circuit photocurrent (I$_{sc}$) is increased by 8 – 9% at normal incidence and at 15°. At higher angles (30° and 45°) the increase is 6 – 7%. The observed enhancement of the photocurrent corresponds to a similar increase in the power conversion efficiency (PCE) at all angles by 6 – 8%.

The AR effect of colloidal silica nanospheres layer with roughly the same diameter (126 ± 13 nm) was demonstrated previously using a small size (16 mm^2) polymer photovoltaic cell (P3HT:PCBM) fabricated on an ITO coated glass substrate [6]. These workers observed a maximum increase of the PCE by 13% at normal incidence of the light. With increasing incident angles the observed increase was slightly reduced. This angular dependence of the PCE for the OPV cell coated with this AR layer is similar to our results presented in Fig. 5.

Fig. 6 presents the I$_{sc}$ and the PCE for the OPV module with the AR layer made from silica nanospheres with a diameter of 50 nm and also for the bare OPV module. The observed increase of the photocurrent at normal incidence and at 15° is 5%, which is smaller than for the OPV module with the AR layer made from 120 nm silica nanospheres. However, one can see that at angles of 30° and 45° the increase rises to

10 – 11%. The corresponding increase of the PCE is 4% at small angles and 8% at 45°. As was mentioned, the observed enhancement of the PCE is limited by recombination losses in the excessively thick active layer of these commercial OPV modules.

For the OPV module covered with the 2D PhC made from 210 nm silica spheres we observed only a small increase (3%) of the photocurrent and PCE at the angle 45° and no increase at small angles of the light incidence, within experimental uncertainty, as demonstrated in Fig. 7.

For the OPV module covered with the 2D PhC made from 350 nm silica spheres we observed a small increase of the photocurrent and PCE at small angles of the light incidence, as expected from optical transmission and reflectance measurements. This is demonstrated in Fig. 8. One can see that at 45° due to light trapping effect in the 2D PhC layer the observed enhancement of the photocurrent is > 7% and the corresponding increase of the PCE is equal to 5%.

2D colloidal PhCs made from larger size silica spheres (> 500 nm) are capable of intrinsic diffractive scattering of the light in the forward direction [29] and can diffractively couple light due to whispering gallery modes [30] that can be used for light trapping in thin film solar cells, for example, a-Si:H [15] and OPVs [31]. With this in mind we investigated light trapping properties of the 2D PhCs made by the R2R LB technique from silica spheres with two different diameters: 600 nm and 740 nm.

Fig. 9 shows the SEM image and the photograph of the 2D colloidal PhC (SiO$_2$ 740 nm) with a total area of 410 cm^2 deposited onto PET foil using the R2R LB technique. The SEM image presents closed packed array of silica spheres demonstrating hexagonal symmetry. On the photograph one can see rainbow colours due to characteristic diffractive scattering of light on the 2D PhC structure.

Optical transmission spectra of the 2D colloidal PhCs made from colloidal silica spheres of diameters 600 nm and 740 nm deposited on PET film (50 µm) are presented in Fig. 10. In both spectra of the 2D PhCs one can see features characteristic for the 2D hexagonal array of silica spheres: the transmission minimum at $\lambda \sim D$ and the strong attenuation at $\lambda \leq D$, where D is the diameter of the spheres. Experimental studies have revealed that the transmission minimum is related to the excitation of surface propagating modes and the resonant coupling of these modes with the incident light [32]. Diffractive scattering of light in the forward direction is responsible for the attenuation observed at $\lambda \leq D$. By analysing transmission spectra at different angles and polarizations of the incident light, it is possible to obtain the photonic band structure of the 2D colloidal PhC [29]. The diffracted angle at the normal incidence can be determined by using the formula: $\sin\alpha = 2\lambda/(d\sqrt{3})$ [13], where d is the nearest neighbour sphere spacing within the plane. As one can see, the 2D array of spheres diffracts light

Fig. 4. Photographs and I-V graphs recorded from the bare OPV module and the OPV module with the AR nanospheres layer (SiO$_2$ 120 nm) deposited by using the R2R LB technique.
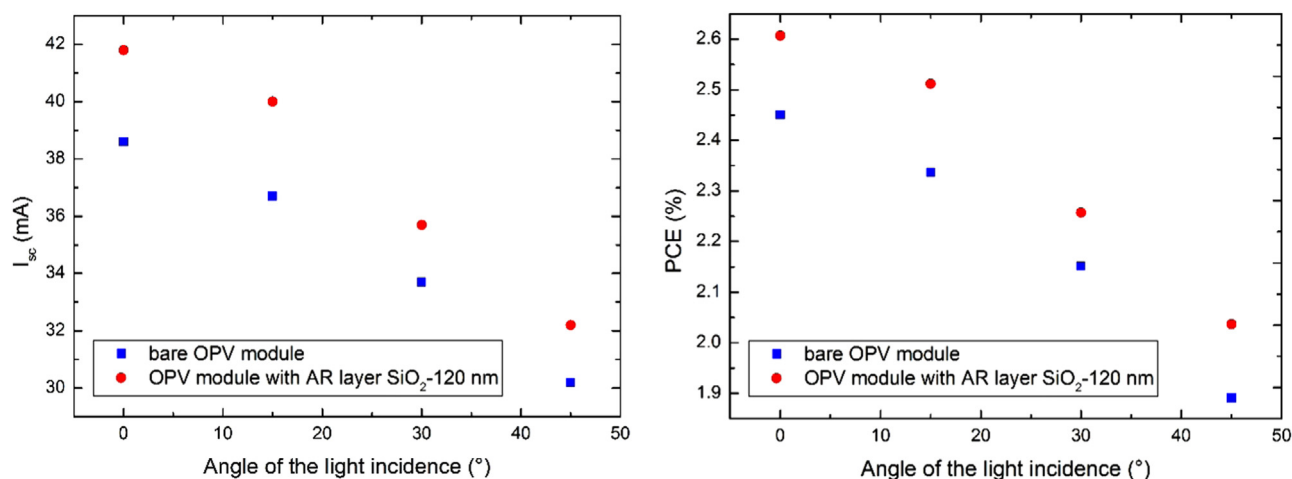
Fig. 5. Angle dependence of the short circuit photocurrent (I_{sc}) and the power conversion efficiency (PCE) for the OPV module with the AR layer (nanospheres SiO$_2$ 120 nm) deposited on PET foil using the R2R LB technique (red circles) and the bare OPV module (blue squares).
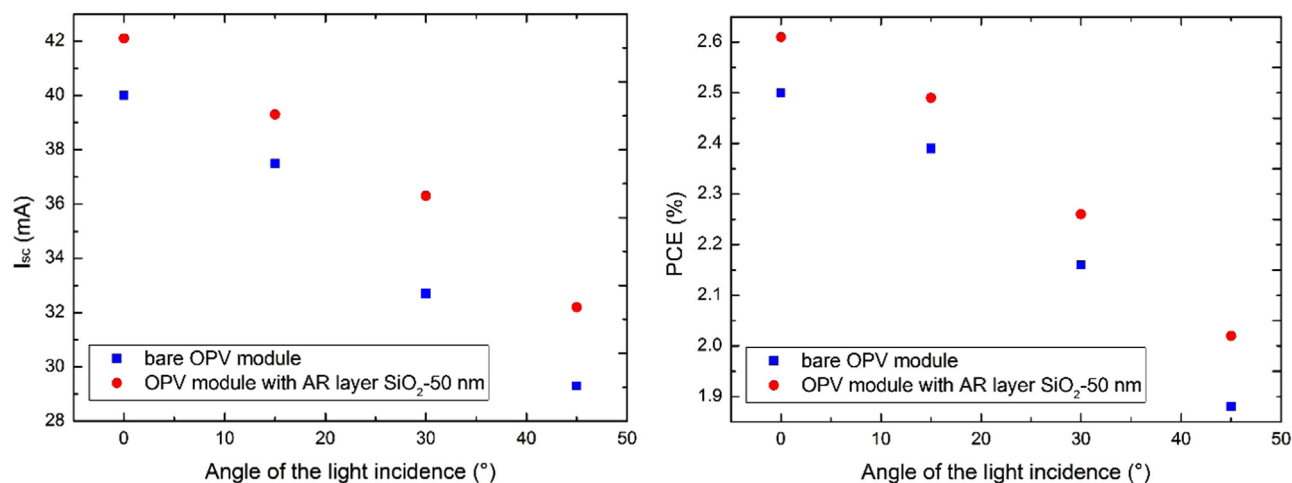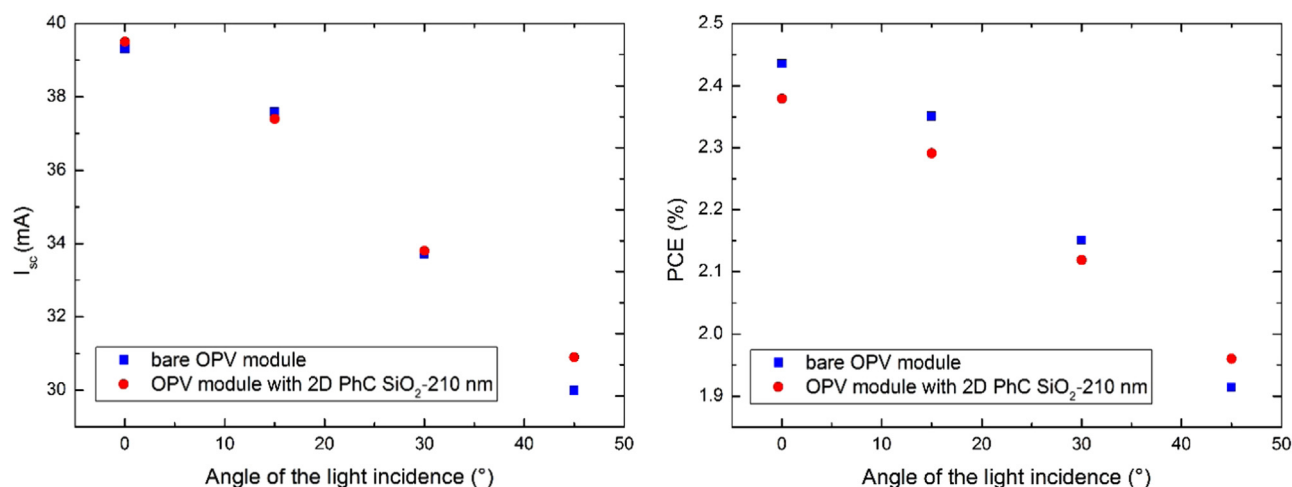

Fig. 6. Angle dependence of the short circuit photocurrent (I_{sc}) and the power conversion efficiency (PCE) for the OPV module with the AR layer (nanospheres SiO$_2$ 50 nm) deposited on PET foil using the R2R LB technique (red circles) and the bare OPV module (blue squares).

Fig. 7. Angle dependence of the short circuit photocurrent (I_{sc}) and the power conversion efficiency (PCE) for the OPV module with the 2D PhC layer (SiO$_2$ 210 nm) deposited on PET foil using the R2R LB technique (red circles) and the bare OPV module (blue squares).

at different wavelengths into specific angles. This effect is clearly seen on the photograph of the 2D colloidal PhC made from silica spheres with a diameter of 740 nm (Fig. 9). For a fixed wavelength the diffracted angle depends on the diameter of closed packed silica spheres. The diffractive scattering will result in an increase of the optical path-length and a corresponding increase of the light absorption in
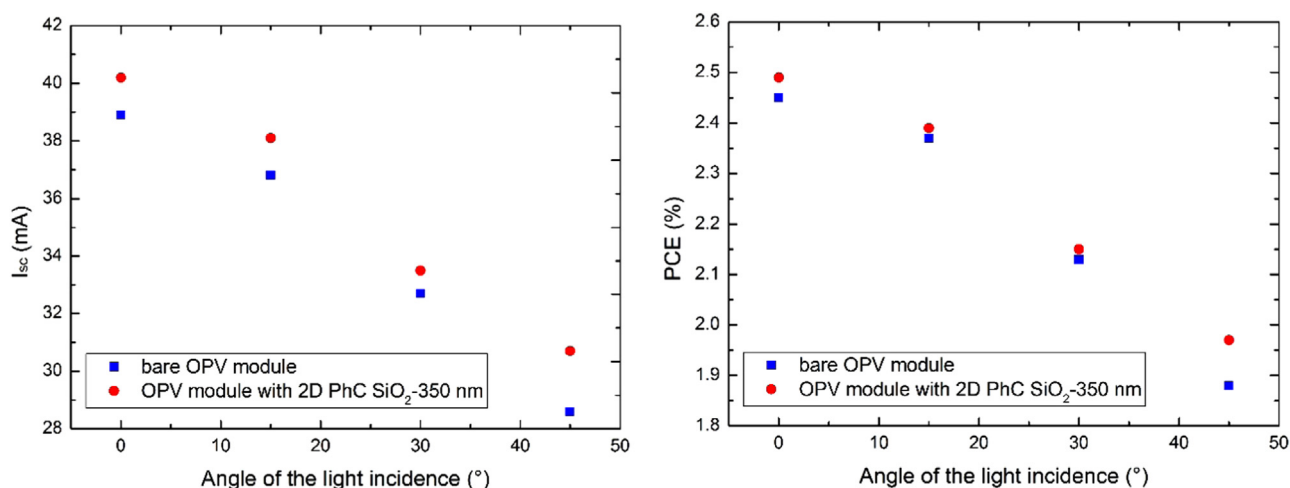
Fig. 8. Angle dependence of the short circuit photocurrent (I_{sc}) and the power conversion efficiency (PCE) for the OPV module with the 2D PhC layer (SiO_2 350 nm) deposited on PET foil using the R2R LB technique (red circles) and the bare OPV module (blue squares).
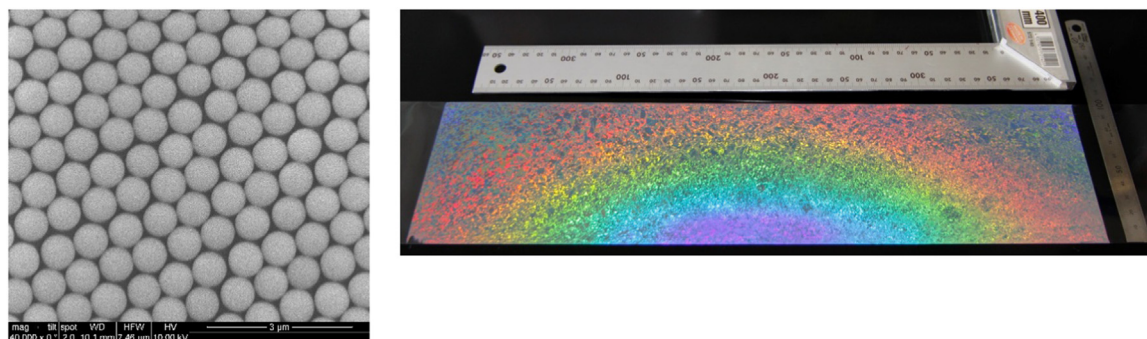

Fig. 9. SEM image and photograph of the 2D colloidal PhC of 740 nm SiO_2 spheres deposited on PET film using the R2R LB technique. The total area is 410 cm^2. The rainbow effect is due to typical diffractive scattering of the flash light on the 2D PhC layer.
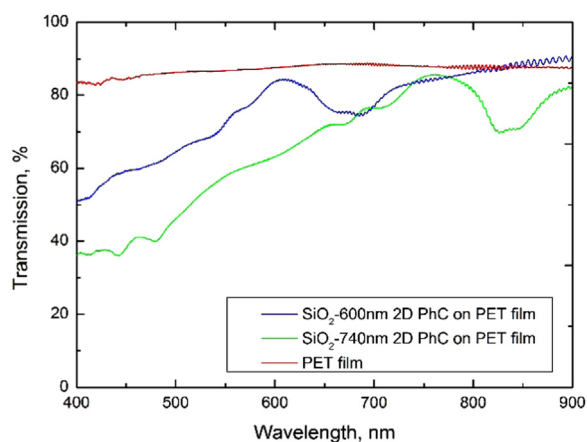

Fig. 10. The transmission spectra of the 2D colloidal PhCs made of silica spheres with diameters of 600 nm (blue line) and 740 nm (green line) deposited on PET film, transmission of the PET film (50 µm) is also shown (red line).

the photoactive layer of OPV cells. There is also another important mechanism for light trapping. It was demonstrated in ref. 30 that whispering gallery modes in the 2D array of silica spheres can effectively couple light inside the photoactive layer of thin film solar cells.

In Fig. 11 one can see a photograph of the OPV module made just after deposition of the 2D colloidal PhC layer of 740 nm SiO_2 spheres and optical transmission spectra of the OPV module with and without the 2D colloidal PhC layer of 740 nm SiO_2 spheres. One can see that the OPV module is optimised for a complete absorption in the spectral

region 550–700 nm (transmission ca. 0%) and therefore, the ability of the 2D PhC layer to increase the absorption of the light in the active layer of the OPV module is limited to the blue and green regions of the solar spectrum. It is interesting to mention that comparing the transmission spectrum of the bare OPV module with the spectrum of the 2D colloidal PhC made from colloidal silica spheres of diameter 740 nm, one can see that diffractive scattering of the light in the 2D PhC is perfectly matched to the absorption band of the OPV module.

Figs. 12 and 13 show the short circuit photocurrent and the power conversion efficiency of the bare OPV modules and the OPV modules with the light trapping layers of the 2D colloidal PhCs made of silica spheres (diameters of 600 nm and 740 nm), measured at different angles of incidence. We observed only a small increase (up to 5%) of the photocurrent and a corresponding enhancement of the efficiency (up to 2%) in the OPV modules due to the PhC light trapping layers. As was mentioned, recombination losses in the active layer is the dominant limiting factor concerning the PCE. It is interesting to note that we observed also a small negative effect for the OPV module with the 2D PhC of 740 nm silica spheres at the high incident angle of 45°. We suggest that this is due to the blue shift of the reflectance peak at higher angles of the light incidence. However, we also note that the positive effect from the 2D PhC light trapping layers could be more evident if the thickness of the photoactive layer could be optimised for the effective charge extraction, as was demonstrated in ref. 30, achieving 13% efficiency enhancement in OPV cells (0.38 cm^2) covered with a layer of silica nanoparticles of diameter 570 nm, while reducing the thickness of the photoactive polymer layer by 30%. In this work, the I_{sc} enhancement of 9% due to the light trapping was observed, which in combination with the FF increase by 2% demonstrated 13.5%
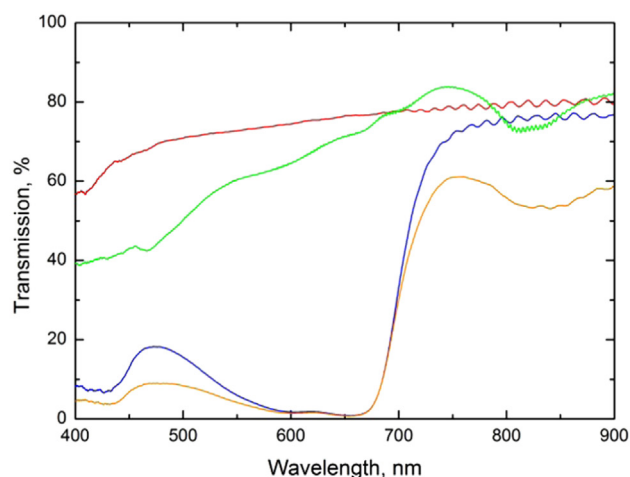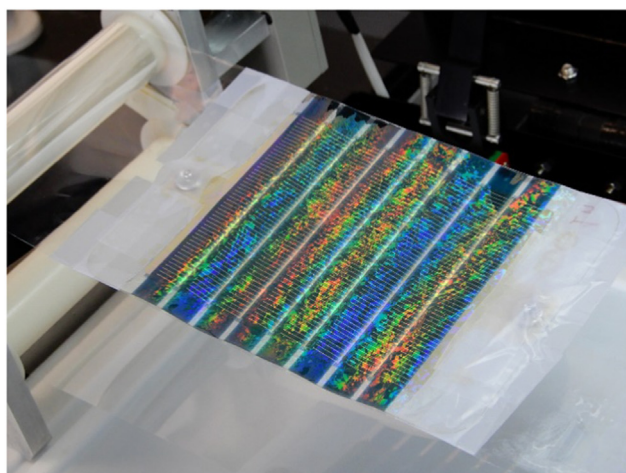
Fig. 11. Left: the photograph of the OPV module after deposition of the 2D colloidal PhC made of silica spheres with a diameter of 740 nm. Right: the transmission spectra of the bare OPV module – PET film and photoactive layer (blue line) and the OPV module with the 2D PhC made of silica spheres with a diameter of 740 nm (orange line); the transmission spectra of the PET film used in the OPV module (red line) and the 2D colloidal PhC made of silica spheres with diameter 740 nm deposited on this PET film (green line) are also shown for the reference.
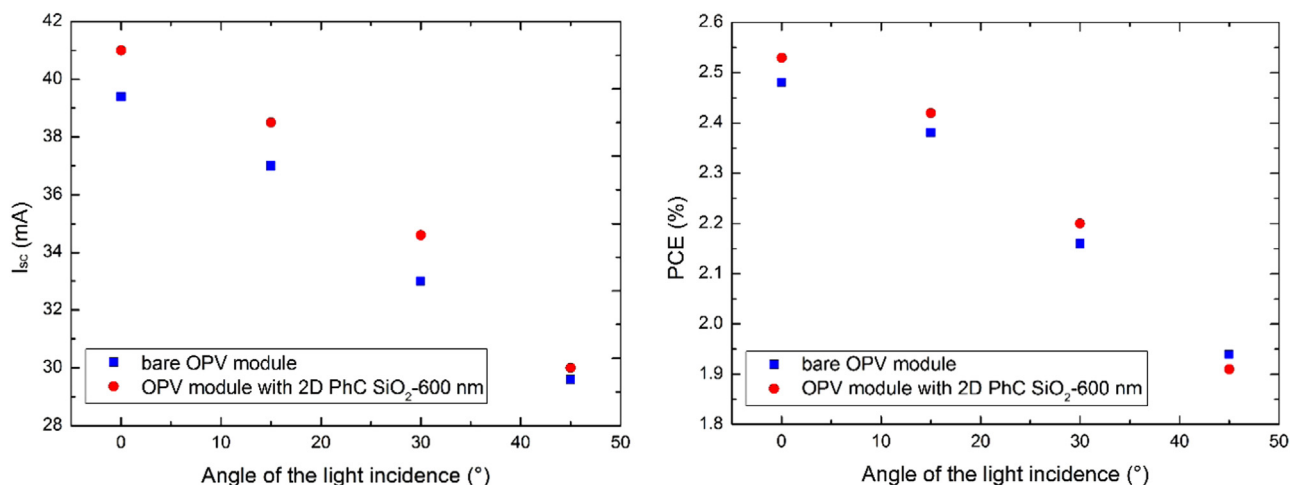

Fig. 12. Angle dependence of the short circuit photocurrent (I_{sc}) and the power conversion efficiency (PCE) for the OPV module with the 2D PhC layer (SiO$_2$ 600 nm) deposited by using the R2R LB technique (red circles) and the bare OPV module (blue squares).
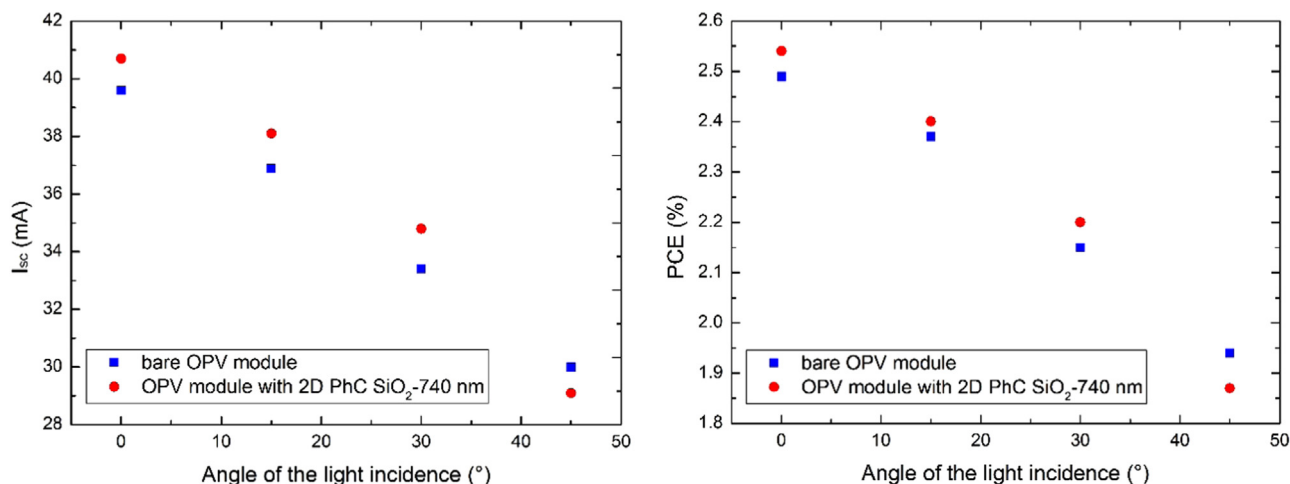

Fig. 13. The power conversion efficiency (PCE) and the short circuit photocurrent (I_{sc}) of the bare OPV module (blue squares) and the OPV module with the 2D colloidal PhC made of silica spheres, diameter of 740 nm (red circles).

enhancement of the PCE. This demonstrates that recombination losses in a thinner active layer will be not a limiting factor for the PCE.

4. Conclusions

For the first time, the application of large-area 2D colloidal PhCs for light trapping in commercial OPV modules is demonstrated via the study of a broad range of light trapping structures deposited simply and cheaply using our novel roll-to-roll Langmuir–Blodgett technique. We have demonstrated that two light trapping effects must be considered when considering the consequences of depositing 2D PhCs on OPV modules – anti-reflection and diffractive light trapping. These are size-dependent phenomena which relate to the fundamental properties of these unique photonic layers. The term unique may genuinely be used here because they do not behave simply as grating structures.

The photonic structures made from silica nanospheres with diameters of 50 nm and 120 nm demonstrated good antireflective properties in VIS-NIR spectral range, resulting in increase of the photocurrent (up to 10%) and the total efficiency in the OPV modules (up to 8%) at all angles of the light incidence. It is interesting to note that the positive effect from the AR layer made of 50 nm SiO_2 nanospheres is increasing for higher angles of the light incidence and for the AR layer made of 120 nm SiO_2 nanospheres this effect drops slightly with increasing incident angles.

We also show that 2D colloidal PhCs made from SiO_2 spheres with diameters of 600 nm and 740 nm possess strong diffractive scattering of the incident light in the forward direction and can also diffractively couple light, which can be used for light trapping in flexible OPV modules. However, we need to mention that if the OPV modules are optimised for complete light absorption, the light trapping effect could be relatively small. The enhancement of the PCE is limited by recombination losses in the thick active layer of these commercial OPV modules. In order to obtain a pronounced positive effect from the light trapping layers made from the 2D PhCs of 600 nm and 740 nm silica spheres, the thickness of the photoactive layer must be optimised for better charge extraction.

We have demonstrated the application of simple cheap technology which is easy scalable, roll-to-roll compatible, and is capable of significantly enhancing the performance of already optimised OPV modules. This has commercial as well as scientific significance.

An additional potential advantage of the technology presented here that large area 2D colloidal PhCs can be used not only as light trapping structures for flexible OPV modules, but also for the light out-coupling in flexible organic light emitting devices (OLEDs). Such experiments are currently on-going in our labs.

Acknowledgements

References

[1] R. Søndergaard, M. Hösel, D. Angmo, T.T. Larsen-Olsen, F.C. Krebs, Roll-to-roll fabrication of polymer solar cells, Mater. Today 15 (2012) 36–49.

[2] L. Lucera, F. Machui, H.D. Schmidt, T. Ahmad, P. Kubis, S. Strohm, J. Hepp, A. Vetter, H.-J. Egelhaaf, C.J. Brabec, Printed semi-transparent large area organic photovoltaic modules with power conversion efficiencies of close to 5%, Org. Electron. 45 (2017) 209–214.

[3] D.-H. Ko, J.R. Tumbleston, A. Gadisa, M. Aryal, Y. Liu, Rene Lopez, E.T. Samulski, Light-trapping nano-structures in organic photovoltaic cells, J. Mater. Chem. 21 (2011) 16293–16303.

[4] Z. Tang, W. Tress, O. Inganäs, Light trapping in thin film organic solar cells, Mater. Today 17 (2014) 389–396.

[5] M. Karg, T.A.F. König, M. Retsch, et al., Colloidal self-assembly concepts for light management in photovoltaics, Mater. Today 18 (2015) 185–205.

[6] W.C. Luk, K.M. Yeung, K.C. Tam, K.L. Ng, K.C. Kwok, C.Y. Kwong, A.M.C. Ng, A.B. Djurišić, Enhanced conversion efficiency of polymeric photovoltaic cell by nanostructured antireflection coating, Org. Electron. 12 (2011) 557–561.

[7] K. Forberich, G. Dennler, M.C. Scharber, K. Hingerl, T. Fromherz, C.J. Brabec, Performance improvement of organic solar cells with moth eye anti-reflection coating, Thin Solid Films 516 (2008) 7167–7170.

[8] S.-I. Na, S.-S. Kim, J. Jo, S.-H. Oh, J. Kim, D.-Y. Kim, Efficient polymer solar cells with surface relief gratings fabricated by simple soft lithography, Adv. Funct. Mater. 18 (2008) 3956–3963.

[9] X.H. Li, W.E.I. Sha, W.C.H. Choy, D.D.S. Fung, F.X. Xie, Efficient inverted polymer solar cells with directly patterned active layer and silver back grating, J. Phys. Chem. C 116 (2012) 7200–7206.

[10] J.-Y. Chen, M.-H. Yu, C.-Y. Chang, Y.-H. Chao, K.W. Sun, C.-S. Hsu, Enhanced performance of organic thin film solar cells using electrodes with nanoimprinted light-diffraction and light-diffusion structures, ACS Appl. Mater. Interfaces 6 (2014) 6164–6169.

[11] D. Duché, C. Masclaux, J. Le Rouzo, C. Gourgon, Photonic crystals for improving light absorption in organic solar cells, J. Appl. Phys. 117 (1–8) (2015) 053108.

[12] J.D. Joannopoulos, P.R. Villeneuve, S.H. Fan, Photonic crystals: putting a new twist on light, Nature 386 (1997) 143–149.

[13] Z. Cai, N.L. Smith, J.T. Zhang, S.A. Asher, Two-dimensional photonic crystal chemical and biomolecular sensors, Anal. Chem. 87 (2015) 5013–5025.

[14] G. Kocher-Oberlehner, M. Bardosova, M. Pemble, B.S. Richards, Planar photonic solar concentrators for building-integrated photovoltaics, Sol. Energy Mater. Sol. Cells 104 (2012) 53–57.

[15] J. Grandidier, R.A. Weitekamp, M.G. Deceglie, D.M. Callahan, C. Battaglia, C.R. Bukowsky, C. Ballif, R.H. Grubbs, H.A. Atwater, Solar cell efficiency enhancement via light trapping in printable resonant dielectric nanosphere arrays, Phys. Status Solidi A 210 (2013) 255–260.

[16] P. Jiang, J.F. Bertone, K.S. Hwang, V.L. Colvin, Single-crystal colloidal multilayers of controlled thickness, Chem. Mater. 11 (1999) 2132–2140.

[17] Y. Fang, B.M. Phillips, K. Askar, B. Choi, P. Jiang, B. Jiang, Scalable bottom-up fabrication of colloidal photonic crystals and periodic plasmonic nanostructures, J. Mater. Chem. C 1 (2013) 6031–6047.

[18] H. Yang, P. Jiang, Large-scale colloidal self-assembly by doctor blade coating, Langmuir 26 (2010) 13173–13182.

[19] A. Coll, S. Bermejo, D. Hernández, L. Castañer, Colloidal crystals by electrospraying polystyrene nanofluids, Nanoscale Res. Lett. 8 (2013) 26.

[20] M. Bardosova, M.E. Pemble, I.M. Povey, R.H. Tredgold, The Langmuir-Blodgett Approach to making colloidal photonic crystals from silica spheres, Adv. Mater. 22 (2010) 3104–3124.

[21] P. Masse, S. Ravaine, Engineered multilayer colloidal crystals with tunable optical properties, Chem. Mater. 17 (2005) 4244–4249.

[22] M.E. Pemble, M. Bardosova, I.M. Povey, R.H. Tredgold, D. Whitehead, Novel photonic crystal thin films using the Langmuir–Blodgett approach, Phys. B 394 (2007) 233–237.

[23] M. Parchine, J. McGrath, M. Bardosova, M.E. Pemble, Large area 2D and 3D colloidal photonic crystals fabricated by a roll-to-roll Langmuir–Blodgett method, Langmuir 32 (2016) 5862–5869.

[24] W. Stöber, A. Fink, E. Bohn, Controlled growth of monodisperse silica spheres in the micron size range, J. Colloid Interface Sci. 26 (1968) 62–69.

[25] S.C. Padmanabhan, J. McGrath, M. Bardosova, M.E. Pemble, A facile method for the synthesis of highly monodisperse silica@gold@silica core-shell-shell particles and their use in the fabrication of three-dimensional metallodielectric photonic crystals, J. Mater. Chem. 22 (2012) 11978–11987.

[26] T. Kohoutek, M. Parchine, M. Bardosova, H. Fudouzi, M.E. Pemble, Large-area flexible colloidal photonic crystal film stickers for light trapping applications, Opt. Mater. Express 8 (2018) 960–967.

[27] A. Deák, I. Székely, E. Kálmán, Zs Keresztes, A.L. Kovács, Z. Hórvölgyi, Nanostructured silica Langmuir–Blodgett films with antireflective properties prepared on glass substrates, Thin Solid Films 484 (2005) 310–317.

[28] A. Deák, B. Bancsi, A.L. Tóth, A.L. Kovács, Z. Hórvölgyi, Complex Langmuir–Blodgett films from silica nanoparticles: an optical spectroscopy study, Colloids Surf. A: Physicochem. Eng. Asp. 278 (2006) 10–16.

[29] T. Yamasaki, T. Tsutsui, Fabrication and optical properties of two-dimensional ordered arrays of silica microspheres, Jpn. J. Appl. Phys. 38 (1999) 5916–5921.

[30] J. Grandidier, D.M. Callahan, J.N. Munday, H.A. Atwater, Light absorption enhancement in thin-film solar cells using whispering gallery modes in dielectric nanospheres, Adv. Mater. 23 (2011) 1272–1276.

[31] J. Yun, W. Wang, S.M. Kim, T.-S. Bae, S. Lee, D. Kim, G.-H. Lee, H.-S. Lee, M. Song, Light trapping in bendable organic solar cells using silica nanoparticle arrays, Energy Environ. Sci. 8 (2015) 932–940.

[32] S.G. Romanov, M. Bardosova, I.M. Povey, M.E. Pemble, C.M.S. Torres, Understanding of transmission in the range of high-order photonic bands in thin opal film, Appl. Phys. Lett. 92 (2008) (191106-1–191106-3).